FAST PARTICLE HEATING

R. Koch, D. Van Eester
Laboratory for Plasma Physics, ERM/KMS,
EUROfusion Consortium member, B-1000, Brussels, Belgium

ABSTRACT

The heating of plasmas by fast ions, with a focus on Neutral Beam Injection (NBI), is reviewed. First, the need of auxiliary heating and current drive systems in fusion machines is outlined. For the particular case of tokamaks, the limitations of Ohmic heating are discussed. The different ways of generating fast particles in plasmas are presented. The principle of operation of neutral beam injectors is explained. Positive-ion (PNBI) and negative-ion (NNBI) based concepts are discussed. Next, the physical processes by which the beam transfers energy to the plasma, namely ionization and slowing-down are described. For both, an elementary theory is given, whereby simple approximations to the distribution functions of beam injected ions and of alpha particles in reactors are obtained. Applications of NBI to heating, current drive and rotation drive are reviewed and the prospects of NBI for ITER are commented.

I. INTRODUCTION

The plasma of a tokamak cannot be heated to ignition using Ohmic heating only because the Joule heating efficiency decreases with the plasma temperature and because the maximum value of the plasma current is limited by the onset of magnetohydrodynamic instabilities that kill the discharge (disruption). These limitations of Ohmic heating will be briefly discussed in the next section. This is the first reason why auxiliary heating systems are required in tokamaks. For steady-state tokamak operation, also the plasma current needs to be sustained by external means, because the inductive current generation is by essence a non-stationary phenomenon. Because the momentum transfer required to generate a current is necessarily accompanied by energy transfer, any non-inductive current-drive method is also a heating method. Specific current-drive aspects will be treated in a subsequent lecture in these proceedings [1]. In other fusion reactor concepts like stellarators, the plasma must be both created and heated by external means. Therefore in all cases, additional heating systems are required. They can also be used for the production of plasma for wall cleaning and conditioning, ramping-up of the plasma current at the beginning of the discharge, tailoring of the plasma current profile in the stationary current phase and inducing toroidal rotation. Some more exotic applications are: inducing a poloidal rotation, influencing fast particle transport or stabilizing MHD modes. The methods allowing doing this are termed "additional heating" methods, although in some cases they constitute in fact the primary or only source of plasma heating.

There are basically two ways of increasing the energy content of the plasma: one can inject either highly energetic particles or electromagnetic energy into the plasma. In both cases the energy must eventually be transferred to the bulk of the plasma and, ultimately to the fuel-ion component to generate the fusion reactions. The thermalization of the externally injected energy usually takes place through collisional processes: the injected fast particle or the particle accelerated by the electromagnetic field transfers its energy to the plasma background by collisions. In a reactor, the alpha particles generated by the fusion reactions also constitute a fast particle population that will heat the plasma by collisions. Therefore heating by fast particles is generic in fusion machines.

II. LIMITATIONS OF OHMIC HEATING

The power dissipated by the current flowing in a tokamak plasma is called "Ohmic Heating" power or "OH" power. It could also be called "Joule heating" as it is due to the dissipation associated with the electrical resistance of the plasma. The plasma current is an electron current and the resistivity is due to the collisions of the conduction electrons with the -essentially immobile- background ions. The resistance of the plasma loop is [2]

$$R_p = \frac{10^{-3} R_o Z_{eff}}{a_p^2 \kappa \gamma_E(Z_{eff})} \Big[1 + (\frac{a_p}{R_o})^{1/2}\Big] T_{e,av}^{-3/2} \qquad (1)$$

where R_o and a_p are the plasma major and minor radii, κ is the elongation, Z_{eff} is the effective ion charge and γ_E is a function of Z_{eff} that can be approximated by

$$\gamma(Z_{eff}) \approx 1 - 0.98/Z_{eff} + 0.56/Z_{eff}^2. \qquad (2)$$

Note that this function takes a value close to 1/2 for clean plasmas. In Eq.1, the factor in square brackets accounts for the trapped particle corrections,

and $T_{e,av}$ is the volume-averaged electron temperature expressed in eV's. Unless explicitly stated otherwise, like above for temperatures, SI units are used throughout the paper. The $T^{-3/2}$ dependence reflects the fact that the strength of the collisions decreases as the cube of the relative velocity between the colliding species. This dependence also implies that the plasma resistance quickly drops as the plasma becomes hotter. The Ohmic power is also proportional to the square of the plasma current (I_p):

$$P_{OH} = R_p I_p^2. \quad (3)$$

So, although the resistance falls down when the current is increased as a result of the plasma heating, it is not clear from the above equations whether the Ohmic power increases or decreases with current. In order to investigate further the consequences of the fall in resistivity, we need a relation linking T_e to I_p. This is available from the so-called scaling laws for tokamaks [3] that provide an expression for the total energy content of the plasma W as a function of the various plasma parameters. In the Ohmic regime, the so-called ITER89 scaling is:

$$W_{OH} = 64 \times 10^3 M^{0.2} I_p^{0.8} R_o^{1.6} a_p^{0.6} \kappa^{0.5} N_{e,LA}^{0.6} B_T^{0.35} \quad (4)$$

where the new parameters introduced are the isotopic mass M and the line-averaged density $N_{e,LA}$. In the above, $N_{e,LA}$ is expressed in $10^{20} m^{-3}$ while the plasma current I_p is expressed in MA. Equating this expression to the definition of the total plasma energy content,

$$W_{OH} = (\kappa \pi a_p^2)(2\pi R_o) 3 N k_B T_{av}$$

in which k_B is the Boltzmann constant, one gets

$$T_{av} = 68 M^{0.2} I_p^{0.8} R_o^{0.6} a_p^{-1.4} \kappa^{-0.5} N_{e,LA}^{-0.4} B_T^{0.35} \quad (5)$$

where T^{av} is in eV. It is amazing to note that because

$$T_{av} \propto I_p^{0.8} \quad (6)$$

the energy confinement time $\tau_E = W_{OH}/P_{OH}$ is independent of the current and the (Ohmic heating) power. This situation, which is characteristic of the good Ohmic confinement, is in strong contrast with the confinement degradation observed in auxiliary heated discharges where

$$\tau_E \propto P_{tot}^{-0.5} \quad (7)$$

However good the Ohmic confinement, Ohmic heating nevertheless is insufficient to bring a large machine to ignition. Using ITER-FDR-type parameters ($R_o = 7.75m$, $a_p = 2.8m$, $\kappa = 1.6$, $I_p = 25MA$, $B_T = 6T$), Eq.(5) implies $T_{av} \approx 1.3keV$. Even taking into account that the temperature profile is peaked, this means that it is difficult to get a central temperature that is high enough to ignite the plasma in Ohmic operation. At first sight, rising the current above 25MA seems to be a solution. However, the plasma becomes magneto-hydrodynamically unstable and disrupts when a too high current flows through it (see [4]). The limiting condition ($q_{edge} > 2$) can be written as

$$I_p[MA] = \frac{5 a_p \kappa B_T}{2 R_o}. \quad (8)$$

Hence, 25MA is about the maximum current that can be obtained in a machine of this size and additional heating is required to bridge the gap to ignition. These conclusions, resting here on very simple considerations, are corroborated by more sophisticated simulations [5].

III. HEATING BY FAST PARTICLES

The basic heat source in a reactor will be the alpha-particles (^4He nuclei) produced by the $D-T$ reaction:

$$D + T \rightarrow^4 He(3.5MeV) + n(14.1MeV)$$

Because of the strong dependence of the fusion reactivity on the ion temperature ($< \sigma_f v > \propto T_i^2$), the fast α-particles are mostly produced in the plasma core. Two additional heating methods are available for producing fast ion populations: NBI and ion cyclotron heating (ICRH). NBI directly injects fast neutrals in the plasma. The injected energy of the electrons is negligible because of their very small mass, so in the end only fast ions matter. ICRH directly accelerates ions inside the plasma at the ion-cyclotron resonance layer. Fast electrons cannot play a role similar to that of ions in heating because their collisionality is very low. In electron cyclotron heating, for example, the perpendicular distribution function remains nearly Maxwellian and the heating power goes through this nearly thermal population. On the other hand, electron cyclotron heating, like lower hybrid heating, can produce a substantial parallel velocity, making it a key player for non-inductive current drive.

IV. NEUTRAL BEAM INJECTION

Because of the strong toroidal magnetic field, there is no possibility to directly inject energetic charged particles inside the plasma. Instead, one injects fast neutrals at the expense of going through the sequence schematically described in Fig.1. The ions are produced in the source and accelerated to a high energy, usually electrostatically, before crossing a charge exchange cell where they are neutralised. The neutralisation is only partial and the remaining ions are deflected magnetically and sent to a dump. Usually, their energy is lost but it is conceivable to recover it by biasing the dump. The neutrals can

then cross the machines magnetic field and reach the plasma where they get ionized, transferring afterwards their energy to the plasma bulk by collisions. The beam source is a plasma discharge from which the ions are extracted by an electrostatic potential. A hydrogenic plasma discharge -for example in deuterium- not only produces atomic ions, D^+ and D^-, but also molecular ions D_2^+, D_3^+. After acceleration at high energy, these ions are neutralized with very different efficiencies. Figure 2 shows that the maximum neutralization efficiency of a gas cell becomes very small for atomic D^+ ions with energies above $200keV$. This is why high energy beam injectors are based on *negative* ion technology. At lower energy, it is more appropriate to use positive-ion based injectors as the production of positive ions is much easier than that of negative ions.

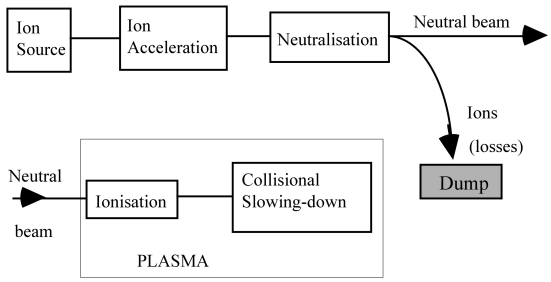

Figure 1: *Sketch of the principle of neutral beam heating. On top, generation of the neutral beam in the injector. Bottom, capture of the neutral beam energy in the plasma.*

A. Neutral beam injectors based on positive ions

All present-day injectors, except one discussed in next section, are based on positive ion (H^+, D^+, ...) technology. Nowadays, neutral beam injectors able to deliver $1-2MW$ of neutrals at energies up to $150keV$ exist. We shall now briefly describe some characteristic features of these injectors. As noted above, the plasma source generates various ion species. After extraction by a negative potential, the negative ions are eliminated but the molecular ions (D_2^+, D_3^+, ...) remain present in the beam. After acceleration and having the same charge, all ions have the same energy, E_o. But, as molecular ions contain several atoms, the final beam of neutrals delivered to the plasma will -after dissociation of molecules and ionization - provide ions at energy $E_o/2$ and $E_o/3$ in addition to the full energy (atomic) beam ions at E_o energy. Some 30% of the total beam power can be carried by these less energetic components that deposit their energy more at the outside of the plasma, as compared to the full energy component. This is a feature that has to be taken into account for computing power deposition profiles. When crossing the neutralization cell, each ion has a neutralization probability that first increases with the length of its path in the cell. Afterwards, neutralized ions can be re-ionized again and the neutralization efficiency decreases [6]. Each ion thus has a maximum neutralization probability for a given thickness of the cell, different for each type of ion. Figure 2 shows this maximum neutralization efficiency. It indicates that for beams with energy below $150keV$, the molecular composition of the beam is that of the source. It also points to the limited efficiency of positive-ion based injectors, which falls below 50% around $100keV$.

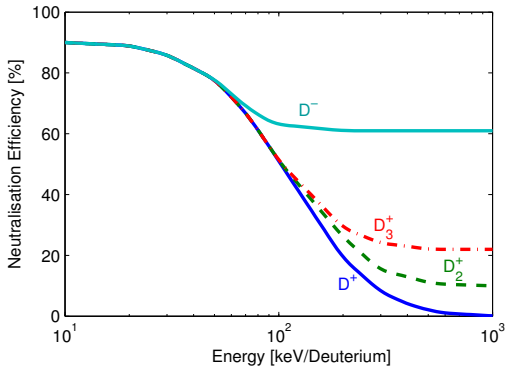

Figure 2: *Maximum neutralisation efficiency in D vs beam energy (see Berkner et al. [6]).*

B. Negative-ion-based injectors

The energy that can be reached -at reasonable efficiency- with positive-ion based technology is insufficient for the next generation of machines. For the heating of the ITER plasma $0.5MeV$ beams are required. If the beams are to be used to non-inductively generate the plasma current, energies of $1-2MeV$ are required. This is clearly out of reach of any positive-ion based neutral beam and efforts are presently devoted to the development of neutral beams based on a negative-ion source.

In their principle, negative-ion beam injectors are identical to the positive-ion based ones, as sketched in Fig. 1. The differences are that (i) the source must preferentially produce negative ions, (ii) negative-ion based beams can operate at much higher energy (0.5 - 1 MeV). The electron captured in the negative ion has a very low binding energy -called affinity- of $0.75eV$. It is therefore very easy to loose, and this feature explains why high neutralization efficiency can be achieved with negative ions (Fig.2). The reverse side of the medal is that these ions are hard to produce. In order to increase their rate of production, one incorporates cesium in the source, an element which has very low ionization potential ($E_1 = 3.894eV$), and which therefore easily liberates electrons. Two production mechanisms are exploited: surface and volume production. In *surface production* the ions are produced when atoms bounce off walls coated with cesium. As intense wall bombardment is required to

get a large negative ion yield, high power densities are required and the initial energy of the negative ions is rather large. Hence the difficulty to operate these sources for long pulses and to produce well focalized ion beams. Volume production rests on a process called dissociative attachment whereby a hydrogen molecule in a high vibrational state breaks up at the time it captures an electron. The efficiency of this mechanism was experimentally found to be unexpectedly large. Nevertheless, the ion yield remained limited, the high gas pressure required leading to early dissociation of the negative ions and high stray electron current. The presently most efficient sources combine both mechanisms through cesium seeding of volume sources. This increases the negative ion yield, minimizes the stray electron current and reduces the isotopic effect. (The production of D^- is only about half that of H^- in volume sources. This is raised to 80% in Cs seeded sources). Standard arc discharge sources have achieved the performances required for ITER [7]. However, they remain complicated and require regular maintenance of the filaments generating the arcs. Therefore a new type of source, the radio-frequency (RF) source, simpler and requiring no maintenance is under development. The status of NBI injector development is described in [8].

Negative ion sources are equipped with extractors that suppress the stray electron current by superposing the field of permanent magnets to the extracting electrostatic field. The stray electrons hit the extractor grid while the negative ion trajectories are nearly unaffected. These ions are then accelerated electrostatically up to energies of the order of the MeV and neutralized. Two types of accelerators are presently under development. The MAMuG (for Multi-Aperture Multi-Gap) accelerates in parallel a number of beamlets in steps of typically $200keV$. On the contrary, the SINGAP combines all beamlets into one single broad beam and provides the acceleration over a single gap. Like for positive ion beams, the simplest neutralization cell is a box filled with gas. At high energy, the maximum efficiency of such a gas neutralizer is about 60% (Fig.2). The adverse mechanism is re-ionization of fast neutrals (producing D^+ or H^+). Theoretically, plasma neutralizers could reach an efficiency of up to 85% if the plasma in the cell is fully ionized. (The efficiency decreases if the plasma is only partially ionized). However the realization of a reliable cell with fully ionized plasma is much more delicate than the gas cell technology.

The target of negative-ion based beam technology is to develop D^0 injectors with, typically, energy of $1MeV$ and a current of $40A$ in order to couple $50MW$ in ITER with three units. The best results have been achieved with the $JT-60U$ injector. This injector was designed for pulses of $10MW$ for $10s$ at $0.5MeV$ [9]. The highest parameters reached up to now with this injector are [10]: $400keV$, $5.2MW$, pulse duration $1.9s$, for D injection; longer pulses have been achieved at reduced power [11]. The neutralization efficiency of 60% has been achieved, in agreement with predictions. More details about the physics of negative-ion beams can be found in a review paper by Pamela [12].

C. Penetration, ionization, losses

Neutral beams are usually injected close to the plasma equatorial plane as this provides the longest path through the densest part of the plasma in front of the beam. With respect to the toroidal direction, beams are usually injected either dominantly parallel or nearly perpendicular. This last solution is technologically easiest but the path through the plasma is rather small and the fast ions are created with large perpendicular energies and therefore a substantial fraction of them can be immediately trapped into banana orbits (see Fig.3). This can lead to significantly larger prompt ion-loss than in the case of parallel injection. Parallel injection beam lines are harder to design because of the limited amount of space available in between the toroidal field coils. However they provide a much longer path for the ionization of the beam and most of the ions are created along passing trajectories. In the parallel injection case, neutrals can be injected in the same direction as the plasma current (co-injection) or in the opposite direction (counter-injection). Due to the asymmetry created by the poloidal field, these two parallel injection schemes are not equivalent. As shown in Fig.3 the orbits of the co-current injected ions drift further outside the magnetic surface on which they were injected than the counter-injected ions. This leads to a somewhat broader power deposition profile in the counter-injection case.

There are two dominant loss mechanisms involved in the energy transfer from the neutral beam to the plasma. (i) Some neutrals cross the plasma without being ionized and are lost on the wall opposite to the injection point. These are called shine-through losses. (ii) Fast ions can get neutralized shortly after their ionization. The so created neutrals will either leave the plasma or be re-ionized at an arbitrary radius. This leads to direct losses and broadening of the power deposition profile. Because the neutralization process is mainly due to charge-exchange (see below), the corresponding losses are called charge-exchange (CX) losses. In the analysis of beam-heated discharges, these losses are usually subtracted from the injected beam power to yield the net power delivered to the plasma taken into account in confinement (power-balance) evaluations. Other losses can occur, especially for non-parallel injection, due to superbanana losses, i.e. loss of banana particles trapped in the ripples of the toroidal magnetic field. Finally if the ions are injected at a velocity faster than the local Alfvén velocity, they can excite global modes - e.g the toroidal Alfvén eigenmodes (TAE) - and be ejected

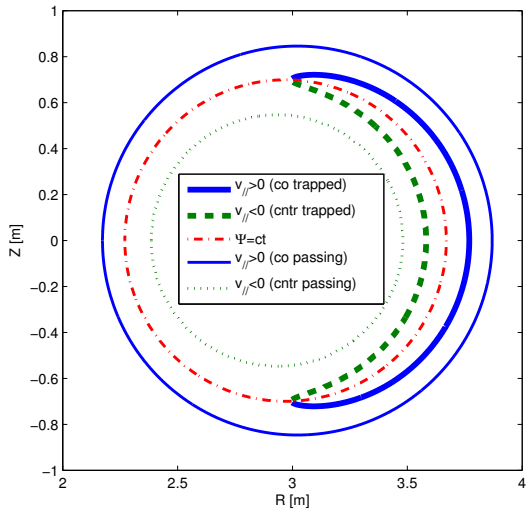

Figure 3: *Poloidal projection of the drift trajectories of beam ions for perpendicular injection (trapped trajectory) and for parallel co- and counter-injection for common toroidal angular momentum and energy; 'co' and 'counter' are defined w.r.t. the plasma current. Also the magnetic surface on which the banana tips lie is depicted.*

out of the plasma by interaction with the TAE's electromagnetic fields.

The ionization of the beam is due to several processes: ionization by impact on electrons and ions (both hydrogenic and impurities), charge exchange and multistep ionization. The dominant process for the lower energy range (e.g. $W_{b0} \leq 80keV$ for deuterons) is charge exchange. The cross-section for charge-exchange with protons was given by Riviere [13] :

$$\sigma_{CX} = 0.6937 \times 10^{-18} \frac{(1 - 0.155 log_{10} E)^2}{1 + 0.1112 \times 10^{-14} E^{3.3}} \quad (9)$$

Here, $E = W_{b0}/M_b$ (in eV/amu) and W_{b0} is the energy of the beam neutral; M_b its isotopic mass number of the beam particles. At higher energy, proton and electron impact ionization become dominant. The cross-section for proton impact is [13]

$$log_{10}\sigma_p = -0.8712(log_{10}E)^2 + 8.156 log_{10}E - 38.833 \quad (10)$$

or

$$\sigma_p = 3.6 \times 10^{-16} log_{10}(0.1666E)/E \quad (11)$$

if $E < 150keV$ or $E > 150keV$, respectively. The cross section for electron impact is [14]

$$\overline{\sigma_e} = < \sigma v_e > / v_{b0} \quad (12)$$

where

$$v_{b0} = 1.3715 \times 10^4 E^{1/2} \quad (13)$$

is the velocity of the neutral and $< \sigma_e v_e >$ is the ionization rate averaged over the electron distribution, which is a function of the electron temperature T_e only. These three cross-sections are represented in Fig.4. If the plasma contains impurities, these can cause additional ionization. The cross-section for ionization by impurities with atomic number Z can be written in terms of a scaled-to-charge cross-section [15]:

$$\sigma_Z = Z\tilde{\sigma}_Z(E/Z) \quad (14)$$

$$\tilde{\sigma}_Z(w) = 7.457 \times 10^{-10} \times \Big[\frac{1}{1 + 0.08095w} + \frac{2.754 ln(1 + 1.27w)}{64.58 + w}\Big] \quad (15)$$

where w is the energy divided by the atomic number expressed in keV. The scaled cross-section $\tilde{\sigma}_Z$ is also represented in Fig.4. In total, the ionization rate per unit length will be

$$-\frac{1}{I_b}\frac{dI_b}{dl} = N_e\sigma_e + N_H\sigma_p + N_H\sigma_{CX} + N_Z\sigma_Z \quad (16)$$

for a H plasma with a single impurity and where we have denoted by I_b the beam intensity and dl the elementary path length along the neutral's trajectory. We define the total or beam-stopping cross-section as:

$$\sigma_0 = \sigma_e + \frac{N_H}{N_e}(\sigma_p + \sigma_{CX}) + \frac{N_Z}{N_e}\sigma_Z \approx \sigma_e + \sigma_p + \sigma_{CX} + \frac{N_Z}{N_e}\sigma_Z. \quad (17)$$

Note, in particular, that the effect of the impurities is proportional to their concentration.

This cross-section was deemed satisfactory for the range of energies typical of early P_{NBI} injection in not too dense plasmas ($N_e \approx 10^{19} m^{-3}$, $E \approx 30 - 40keV$). However, when the injection energy becomes larger, which is typically the case with NNBI, and/or for larger densities, this formula underestimates the cross-section because it ignores multi-step ionization. This is the process by which a neutral first gets into excited states due to successive collisions before being ionized. This process is negligible for a (relatively) slow neutral in low density plasma because the lifetime in the excited state is much shorter than the time between two successive collisions. If the speed of the neutral or the number of particles per unit volume increases sufficiently, this is no longer the case. Multi-step ionization can be taken into account by introducing the beam stopping increment δ_{ms} into the complete cross-section σ

$$\sigma = (1 + \delta_{ms})\sigma_0. \quad (18)$$

The complete cross-sections have been computed by Janev et al. [15], and more recently by Suzuki et al. [16]. These authors also provide analytic fits to the data. The correction due to multi-step ionisation can go to 100% or more for NNBI [17]. For P_{NBI}, the

correction is usually less than 20%. The mean-free path of the neutrals in a plasma of density N is

$$\lambda = 1/(N\sigma) \tag{19}$$

and the evolution of the neutral density $I_b(l)$ for a narrow beam follows from Eq.16:

$$I_b(l) = I_{b0} exp[-\int_0^l dl\sigma(\vec{x})N(\vec{x})] \tag{20}$$

where the integration is along the path $\vec{x}(t)$ of the neutral in the plasma.

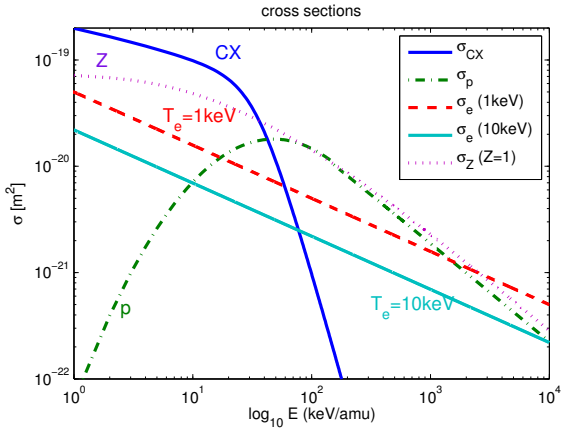

Figure 4: *Cross sections for ionization of fast neutrals by charge-exchange (CX), electron impact (for two different electron temperatures $T_e = 1keV$ and $10keV$), and by proton impact (p). The curve Z is the normalized $\tilde{\sigma}$ for impurities.*

Once created, the ion will follow a trapped or passing orbit, as already discussed. If the confinement of fast particles in the machine is sufficiently good, the ion can be assumed to stay on its magnetic surface and to slow down there by collisions. In a first approximation it is thus sufficient to study the slowing-down process as if it was taking place in an infinite homogeneous plasma having the same parameters as those of the magnetic surface. Neoclassical effects can be taken into account by the so-called bounce-averaging [18] procedure over the real drift-trajectories of particles but this topic will be left out in the present elementary presentation.

V. FAST ION HEATING AND SLOWING DOWN

Given a fast ion content in the plasma, and irrespective of the way it was generated, the transfer of its energy to the plasma bulk can be described in a first approximation as a slowing-down process in homogeneous plasma. This can be examined through two complementary approaches: the test-particle and the Fokker-Planck ones. The latter allows computing the fast-ion distribution function.

A. Slowing down; test particle approach

Starting from the theory of binary Coulomb collisions Sivukhin [19] has shown that the energy decrease of a particle due to the background species s with Maxwellian distribution

$$f_s(v) = \frac{1}{[(2\pi)^{1/2}v_{th,s}]^3} exp[-\frac{v^2}{2v_{th,s}^2}] \tag{21}$$

where $v_{th,s} = (k_B T_s/m_s)^{1/2}$ is

$$\frac{dW_b}{dt} = -\frac{4\pi Z_b^2 e^2}{v_b}\sum_s N_s Z_s^2 e^2 ln\Lambda \left[\frac{Erf(w_s)}{m_s} - \frac{2w_s(m_s+m_b)}{m_s m_b \pi^{1/2}} e^{-w_s^2}\right] \tag{22}$$

with $w_s = v_b/2^{1/2}v_{th,s}$ and the index 'b' refers to the beam ions. Consider a background plasma with ions ($s = i$) and electrons ($s = e$). For a $5keV$ plasma, for example, the thermal electron velocity $v_{th,e}$ is in the range of $3 \times 10^7 m/s$ while $v_{th,i} = 5 \times 10^5 m/s$. A $100keV$ ion has a velocity of $3 \times 10^6 m/s$. Therefore it is usually justified to make the assumption that the injected ions are much slower than the average electron ($w_e \ll 1$) and much faster than the average ion ($1 \ll w_i$). This simplifies considerably Eq.22 as $Erf(x) \approx 2x/\pi^{1/2}$ for $x \ll 1$ and $Erf(x) \approx 1$ for $1 \ll w$. One gets

$$\frac{dW_b}{dt} \approx -\frac{2W_b}{\tau_s}\left[1 + \left(\frac{W_c}{W_b}\right)^{3/2}\right] \tag{23}$$

where the first term in the square brackets corresponds to energy transfer to the electrons and the second one to the background ions. When $W_c = W_b$ an equal amount of power is transferred to electrons and ions. W_c is the critical energy $m_b v_c^2/2$; the critical velocity v_c is given by

$$v_c = (2k_B T_e/m_e)^{1/2}\left[\frac{3\pi^{1/2}}{4}\sum_i \frac{N_i}{N_e} Z_i^2 \frac{m_e}{m_i}\right]^{1/3} \tag{24}$$

yielding

$$W_c = \frac{1}{2}m_b v_c^2 = 14.8 T_e[keV] m_b \Big(\sum_i \frac{N_i Z_i^2}{N_e m_i}\Big)^{2/3}. \tag{25}$$

When the beam ion velocity is much larger than the critical velocity ($W_c \ll W_b$), Eq.(19) is even simpler,

$$\frac{dW_b}{dt} \approx -\frac{2W_b}{\tau_S} \tag{26}$$

which describes a simple exponential decay. In this case all the energy is transferred to the electrons. Note that for the α particles ($M_\alpha = 4$, $Z_\alpha = 2$, $W_{\alpha 0} = 3.5MeV$) generated in a thermonuclear plasma ($T_e \approx 10keV$) one has

$$(W_c/W_\alpha)^{3/2} \approx 10^{-2} \tag{27}$$

implying that α-particles, in a reactor, will heat the electrons rather than the ions. In the case of dominant electron slowing-down the characteristic energy decay time is $\tau_S/2$. τ_S is called the slowing-down time on electrons and is given by the expression

$$\tau_S = \frac{3(2\pi)^{3/2} m_e m_b \epsilon_0 v_{th,e}^3}{N_e Z_b^2 e^4 ln\Lambda} \approx 0.012 \frac{(T_e[keV])^{3/2} M_b}{N_e[10^{20} m^{-3}] Z_b^2} \tag{28}$$

when assuming $ln\Lambda = 16.5$. Rather than being a constant, the latter quantity is a weak function of density, temperature charge and mass. For a $40keV$ deuteron in a $1keV$, $5 \times 10^{19} m^{-3}$ TEXTOR plasma, this gives $\tau_S \approx 50ms$. For an α particle in a $10keV$, $10^{20} m^{-3}$ plasma $\tau_S \approx 400ms$. At this point it should be noted that these values are not far from the energy confinement time values. Therefore, transport can play a role on the same time-scale as slowing-down in the process of energy transfer from the beam to the plasma (or from the α-particle to a reactor plasma).

The above equations describe the instantaneous slowing down of an ion in the plasma. Two other important quantities that describe the whole slowing-down process, from birth velocity to thermal velocity, are the fraction of the total energy that has gone to electrons (F_e) and to the ions (F_i) after complete slowing-down. This is easily evaluated from Eq.23. The instantaneous power transferred to the ions is:

$$P_i = \frac{2W_b}{\tau_S} \left(\frac{W_c}{W_b}\right)^{3/2} \tag{29}$$

and the energy transferred to the ions during the whole slowing-down process is

$$W_i = \int_0^\infty P_i dt. \tag{30}$$

Noting that one can re-write Eq.23 as

$$-\frac{2}{\tau_S} dt = \frac{dy}{y(1 + y^{-3/2})} \tag{31}$$

with $y = W_b/W_c$, one finds

$$\begin{aligned} F_i &= -\frac{1}{W_{b0}} \int_0^\infty W_b \left(\frac{W_c}{W_b}\right)^{3/2} \left(-\frac{2}{\tau_S}\right) \\ &= \frac{W_c}{W_{b0}} \int_0^{W_{b0}/W_c} \frac{dy}{1 + y^{3/2}} \end{aligned} \tag{32}$$

for the ratio $F_i = W_i/W_{b0}$ of the energy W_i collisionally lost to the ions to W_{b0}, the energy at which the beam is injected. The fraction flowing to the electrons then is

$$F_e = 1 - F_i. \tag{33}$$

A plot of these fractions is given in Fig.5.

B. The beam distribution function

The starting point of a computation of the distribution function is the Fokker-Planck equation. Its

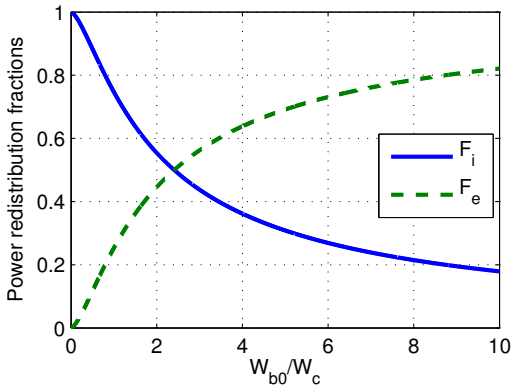

Figure 5: *Fractions F_e and F_i of the beam ions energy going respectively to electrons and to ions during the slowing down process.*

derivation can be found in Sivukhin [19]. This equation can be written:

$$\frac{\partial f_\alpha}{\partial t} = \sum_{\beta \neq \alpha} C(f_\alpha, f_\beta) + C(f_\alpha, f_\alpha) + S - L \tag{34}$$

where $C(f_\alpha, f_\beta)$ is the collision integral for particles of type α and β. The first sum is over all the background plasma species and the 2nd term accounts for collisions among the beam particles themselves. Usually one uses the Landau form of the collision integral [20],

$$C(f_\alpha, f_\beta) = \frac{Z_\alpha^2 Z_\beta^2 e^4 ln\Lambda_{\alpha\beta}}{8\pi\epsilon_0^2 m_\alpha}$$
$$\nabla_{\vec{v}} . \int d\vec{w} \frac{u^2 \overline{\overline{1}} - \vec{u}\vec{u}}{u^3} \Big[\frac{f_\beta}{m_\alpha} \nabla_{\vec{v}} f_\alpha - \frac{f_\alpha}{m_\beta} \nabla_{\vec{w}} f_\beta \Big], \tag{35}$$

as starting point. Here $\vec{u} = \vec{v} - \vec{w}$ and $\overline{\overline{1}}$ is the identity matrix. S is the source of fast ions (beam ions or α-particles; fast ions generated by ICRH do not appear as a source term in Eq.34, but are generated by an additional RF-induced diffusion term, as we shall see in a subsequent lecture). Because the collision operator conserves the number of particles, a loss-term L has to be included, otherwise, there could be no stationary solution to Eq.34. The simplest particle loss-term is

$$L = \frac{f_\alpha}{\tau} \tag{36}$$

which corresponds to both particle and energy loss. With a τ independent of velocity, it constitutes a good representation of charge-exchange losses. A more sophisticated loss term distinguishing particle and energy loss is

$$L = \frac{f_\alpha}{\tau_p} - \frac{1}{v^2} \frac{\partial}{\partial v} \Big[\Big(\frac{1}{\tau_E} - \frac{1}{\tau_p} \Big) \frac{v^3}{2} f_\alpha \Big] \tag{37}$$

where τ_E and τ_p are the energy and particle confinement times, which can be functions of the velocity. Solving Eq.34 is a complex problem because it involves three-dimensional collision integrals

that, even numerically, are heavy to evaluate [20]. In addition, this equation is non-linear because of the beam self-collision term $C(f_\alpha, f_\alpha)$. In order to simplify the problem one can assume (i) that self-collisions are negligible when the beam component is not a too large fraction of the plasma population (ii) that the beam distribution function is independent of the gyro-angle, (iii) that all background species are isotropic Maxwellians. In this case, all the collision integrals can be performed analytically and one arrives at the linear collision operator

$$C(f) = -\frac{1}{v^2}\frac{\partial}{\partial v}(A(v)v^2 f) + \frac{1}{2v^2}\frac{\partial^2}{\partial v^2}(B(v)v^2 f) + \frac{1}{4v^2}\frac{\partial}{\partial \mu}\Big[G(v)(1-\mu^2)\frac{\partial f}{\partial \mu}\Big] \quad (38)$$

expressed in terms of the particle velocity v and of $\mu = v_{//}/v$, the cosine of the pitch-angle. A, B and G are analytic expressions involving the error function [21]. These expressions can be further simplified by assuming, as was done above in the test-particle approach, that $v_{th,i} \ll v_\alpha \ll v_{th,e}$. One then arrives at the limits:

$$-Av^2 + \frac{1}{2}\frac{\partial}{\partial v}(Bv^2) \approx \frac{1}{\tau_S}(v^3 + v_c^3) \quad (39)$$

$$B \approx \frac{2T_e}{m_\alpha \tau_S}(1 + \frac{v_B^3}{v^3}) \quad (40)$$

$$G \approx \frac{v_G^3}{\tau_S v} \quad (41)$$

where one recognizes the earlier defined slowing-down-time τ_S and the critical velocity v_c. The additional expressions for v_B and v_G are [21]:

$$v_B^3 = \frac{3\pi^{1/2}}{4}\Big(\frac{2k_B T_e}{m_2}\Big)^{1/2}\sum_i \frac{N_i}{N_e}Z_i^2\frac{2k_B T_i}{m_i} \quad (42)$$

$$v_G^3 = \frac{3\pi^{1/2}}{4}\frac{m_e}{m_\alpha}\Big(\frac{2k_B T_e}{m_2}\Big)^{1/2}\sum_i \frac{N_i}{N_e}Z_i^2 \quad (43)$$

Finally, retaining only the dominant terms one arrives at the standard form of the collision operator used for the investigation of fast-ion distribution functions:

$$C_1(f) = \frac{1}{\tau_S v^3}\Big[v\frac{\partial}{\partial v}[(v^3+v_c^3)f_\alpha]\Big] + Z_2\frac{\partial}{\partial \mu}\Big[(1-\mu^2)\frac{\partial f_\alpha}{\partial \mu}\Big] \quad (44)$$

with

$$Z_2 = \frac{\sum_i N_i Z_i^2/m_\alpha}{\sum_i N_i Z_i^2/m_i} \quad (45)$$

It is important to note that while the original Landau form Eq.35 and the linearized form for Maxwellian background Eq.38 conserve the number of particles, the collision operator Eq.44 does not. Therefore the classical Fokker-Planck equation for fast ions can be written omitting a loss term:

$$\frac{\partial f_\alpha}{\partial t} = C_1(f_\alpha) + S. \quad (46)$$

The origin of the loss can be investigated by computing the evolution of the particle density

$$N_\alpha = \int d\vec{v} f_\alpha \quad (47)$$

due to the collision operator C_1 for an isotropic distribution function $f_\alpha(v)$:

$$\frac{\partial N_\alpha}{\partial t}\Big|_{Coll} = 2\pi\int_{-1}^{+1} d\mu \int_0^\infty dv v^2 \frac{\partial f_\alpha}{\partial t}\Big|_{Coll} = -\frac{4\pi v_c^3}{\tau_S} f_\alpha(0) \quad (48)$$

This result states that the origin of velocity space constitutes a particle sink when the C_1 collision operator is adopted.

Equation 46 with $S = 0$ is separable and the eigenfunctions of the pitch-angle operator (the last term in Eq.44) are Legendre polynomials. Therefore an analytic solution of the stationary version of Eq.46 can be obtained for a delta function source [22]

$$S(v,\mu) = \frac{S_0}{v^2}\delta(v - v_{\alpha,0})\delta(\mu - \mu_{\alpha,0}) \quad (49)$$

where S_0 is the rate of injection of the beam particles. The index '$\alpha, 0$' refers to the initial properties of the injected ions. The distribution function can be written:

$$f_\alpha(v,\mu) = \frac{\tau_S S_0}{v^3 + v_c^3}\sum_{l=0}^{\infty}\frac{2l+1}{2}P_l(\mu_{\alpha,0})P_l(\mu) \Big[\frac{v^3}{v_{\alpha,0}^3}\frac{v_{\alpha,0}^3 + v_c^3}{v^3 + v_c^3}\Big]^{(l+1)Z_2/6} H(v_{\alpha,0} - v) \quad (50)$$

where H is the step function. One notes that this distribution function is abruptly cut off at the injection velocity $v = v_{\alpha,0}$ whereas, in reality, some beam ions will be diffusing to velocities in excess of $v_{\alpha,0}$. This is a consequence of the neglect of diffusion by thermal electrons. The characteristics of beam distribution functions have been illustrated in [23].

This obtained distribution function takes a particularly simple form when the source is *isotropic*,

$$S(v) = \frac{S_0}{v^2}\delta(v - v_{\alpha,0}). \quad (51)$$

Whereas this is usually not very realistic for neutral beam injection [23], it is quite appropriate for computing the distribution function of fusion-generated α-particles. For $\partial\mu/\partial\mu = 0$, Eq.46 is particularly easy to solve and one obtains

$$f(v) = \frac{\tau_S S_0}{v^3 + v_c^3}H(v_{\alpha,0} - v). \quad (52)$$

This is a good approximation of the α-particle distribution function and one should note that this function is very different from a Maxwellian. At large velocity, it decays like $1/v^3$ rather than exponentially, and becomes flat below the critical velocity v_c. Although insufficient for modeling the full distribution

function of a beam, the isotropic part of Eq.50 can be used to study quantities only involving the isotropic component.

In the general case of non-isotropic beam injection the beam component of the plasma will contribute to the parallel ($W_{//}$) and perpendicular ($W_{\perp}$) energy content of the plasma differently from the background species for which $W_{\perp} = 2W_{//}$. This has an impact on the interpretation of the diamagnetic and equilibrium energy signals. At the lower densities the beam component can be an appreciable fraction of the total plasma energy content. Similarly, in the reactor, the fast fusion products can contribute significantly to the total plasma beta.

VI. NBI: COMPARISONS WITH EXPERIMENTS

The experimental verification of the two basic processes of beam heating, namely ionization and slowing-down, is not trivial because both processes depend on a number of plasma parameters and profiles. In all what precedes, we have considered the beam as a thin mono-energetic pencil of neutrals. This is not quite the case as the beam cross-section may be a substantial fraction of the poloidal cross-section of the plasma itself. Therefore, a realistic beam can be conceived as a number of parallel thin beamlets, each making its own path through the density, temperature and impurity concentration profiles. Ionization is the easiest to check, by measuring the shine-through of the beam.

A. Ionization

In the already quoted ITER work [17], the theoretical increment in stopping cross-section, due to multi-step ionization is compared with experimental results for both positive and negative NBI in TFTR and JT-60, showing satisfactory agreement. Additional beam shine-through comparisons made in JT-60 can be found in Suzuki [16] and Oikawa [10].

B. Slowing down

Obviously, checks of slowing-down are more indirect as the slowing down computation must start from the result of the ionization computation, i.e. the beam-ion birth profile. For P_{NBI}, the analysis of fast-ion tails is further complicated by the presence of half and third energy beam components (section IV.A). On the experimental side, the direct measurement of fast ion distribution functions inside the plasma is presently not available. One can look at the distribution of the charge-exchange neutrals coming out of the plasma. However, this signal has a simple interpretation only in the case of rather small plasmas of low density, otherwise too few fast neutrals generated in the plasma bulk reach the plasma outside, all others being re-ionized. Comparisons based on charge-exchange spectra were made on PLT, showing good agreement between theory and experiment [24]. Another way of looking at tails is by measuring the neutron rate from $D-D$ reactions (or from other fusion reactions, e.g. $D-T$ if tritium is present). The fusion reaction rate is indeed very sensitive to tails as it peaks in the hundreds of keV range. It is however even more indirect than CX neutrals measurement as the deuterium density and temperature profiles enter once more the computation of the reaction rate. After an abrupt switch-off of the NBI, the fast ion tail remains for a while, decaying at the slowing-down time rate (appropriately averaged over the plasma volume) and so does the neutron production rate. The decay rate of the fusion neutrons is thus an indirect measurement of the slowing-down time. Comparisons have been made in several machines [9, 24, 25], always giving good agreement with predictions.

An even more global way of making comparisons, which has become more or less standard, is to run a transport code equipped with a beam simulation package and to predict the total neutron flux from beam-target (the subject of the comparisons discussed just above), beam-beam and thermal fusion reactions and compare it with the experimentally measured flux [26].

VII. PHYSICS RESULTS WITH NBI

A. Heating

NBI has been used in all major tokamaks in the world and has produced high temperature and high performance plasmas [27, 28]. Shots with NBI heating constitute a large fraction of the ITER database [29]. NBI has also been used with success in $D-T$ experiments [30]. Both D and T have been injected in a $D-T$ target plasma. The highest fusion power output ($16.1MW$) shot in JET was obtained with $3.1MW$ of ICRH power and $22.3MW$ of beam power (with injection of $155keV$ T and $80keV$ D). It must be noted that most shots of this database are P_{NBI} shots with a large fraction of the power coupled to bulk ions because of the relatively low injection energy. For a $1MeV$ NNBI in ITER, the fraction coupled to ions will be much smaller. One should note also that injection energies are often close to the optimum energy for the $D-T$ reaction. For example, for the record JET shot cited above, close to 40% of the reaction rate was due to beam-target reactions. This will no longer be the case in ITER.

B. Current drive

Efficient current drive has also been achieved with NBI [1]. For central current drive, the results with NNBI on JT-60U showed good agreement with the predicted driven current deposition profile [17, 31] and a current drive efficiency somewhat higher than

PNBI [10]. However, recent high power off-axis NNBI did not produce the expected current and q profile changes [32]. This question remains under investigation.

C. Toroidal rotation drive

When a fast neutral particle with speed $\vec{v}_{\alpha,b}$ is ionized, it adds its toroidal angular momentum

$$\Delta L_T = m_\alpha R_b \vec{v}_{\alpha,b}.\vec{e}_{tor} \quad (53)$$

to the plasma. Here $\vec{e}_{tor}$ is the unit vector in the toroidal direction and R_b is the birth radius of the ion; recall that the toroidal angular momentum $L_T = mRv_\varphi - q\Psi/2\pi$ (Ψ being the poloidal flux) is a constant of the motion of a charged particle in an axisymmetric tokamak in absence of collisions. As shown experimentally in JET [33], this addition to the angular momentum will be transferred to the bulk plasma on three different time scales: (i) The ion that is born on a trapped trajectory, looses its momentum on a bounce time-scale. This momentum is transferred to the bulk plasma on the same time-scale by a $\vec{j}\times\vec{B}$ force due to the radial current associated with the displacement of the ion between its birth radius and the average radius of its banana orbit. (ii) The ion that is born on a passing trajectory will transfer its momentum by slowing down on the bulk plasma on a slowing down time scale. (iii) When the passing ion becomes part of the thermal population after full slowing down, it carries its residual toroidal momentum. The associated torques are balanced by toroidal momentum damping, which has been found to be anomalous. It is indeed much larger than the neoclassical estimates, and is usually close to the energy confinement time.

NBI can be used in ITER to induce toroidal rotation in addition to its obvious role of heating and current drive system. However, for high energy injection, the injected momentum per unit power ($\propto 1/v_{\alpha,0}$) is much less than for present experiments with PNBI.

VIII. PHYSICS OF BURNING PLASMAS

With the advent of ITER, a topic that is gathering importance is that of burning plasmas. These are plasmas containing a substantial fraction of fast α particles and in which a significant part of the heating is provided by these ions. As the burning plasma behaves in a more or less self-organized way, its control becomes more difficult, in particular with respect to pressure- or q-profiles. The inhomogeneous and non-Maxwellian fast ion distributions may also feed instabilities, like toroidal Alfven eigenmodes (TAE). When the amplitude of the latter becomes sufficient, the fast particles can get trapped in the wave wells and increased diffusion or loss of fast particles may result. In the strongly nonlinear regimes, coherent wave-particle structures known as energetic particle modes (EPM) can move through the plasma and lead to further fast ion losses [31]. In ITER or in a reactor these phenomena may lead to reduction of the efficiency of α-particle heating and decrease in reactivity. Burning plasma phenomena can to some extent be simulated in present machines using NBI, ICRH or a combination of both. New γ ray and neutron tomography diagnostics have allowed unprecedented measurements of fast ion distributions in the plasma [34, 35].

IX. FURTHER READING

A good introduction to Coulomb relaxation and to the analysis of beam heating of plasmas can be found in the book by Dnestrovskii & Kostamarov [36]. Detailed analysis of Coulomb collisions can be found in the works by Sivukhin [19] and Karney [20]. A technology-oriented description of NBI is given by Kunkel [37]. All the physics that is involved in tokamaks, reactors and ITER can be found in the rather complete ITER Physics Basis [17] and its recent complement Progress in the ITER physics basis [31].

REFERENCES

1. E. WESTERHOF, Current Drive: NBI & RF, these proc.
2. Koch R., Messiaen A.M. and Weynants R.R., LPP-ERM/KMS Brussels Report no 69 (1980)
3. P.N.YUSHMANOV et al., Scalings for tokamak energy confinement, Nucl. Fus. 30, 1999 (1990)
4. R. KOSLOWSKI, Operational limits in tokamak machines and limiting instabilities, these proc.
5. R. KOCH & D. VAN EESTER, Enhancement of reactivity by RF, Plasma Phys. and Contr. Fus. 35A, A211 (1993), F. LOUCHE, R. KOCH, Final Report on ITER subtask D350.1: Modelling of ICRH system heating performances with PION/PRETOR package, LPP-ERM/KMS Brussels Report n115 (1999)
6. K.H. BERKNER et al., Intense, mixed-energy hydrogen beams for CTR injection, Nucl. Fus. 15, 249, (1975)
7. ITER Final Design Report (July 2001)
8. T. INOUE et al., R&D on a high energy accelerator and a large negative ion source for ITER, Nucl. Fus. 45, 790 (2005); V. ANTONI et al., Technological aspects of the different schemes for accelerator and ion source for the ITER neutral beam injector, 21st IAEA Fusion Energy Conference, Chengdu, (2006)IT/2-3Rb; [Older ref:

H.D. Falter et al., Status and plans for the development of an RF negative ion source for ITER NBI, 20th Fusion Energy Conference, Vilamoura (2004) IAEA-CN-116 /FT /12Rc]

9. K. USHIGUSA & JT-60 TEAM, Steady state operation research in JT-60U, Proc. 16-th IAEA Fus. Energy Conf., Montral, IAEA Vienna, Vol.1, 37 (1996)

10. T. OIKAWA, et al., Heating and non-inductive current drive by negative-ion based NBI in JT-60U, Proc. 17-th IAEA Fusion Energy Conference, Yokohama, IAEA Vienna, paper IAEA-F1-CN-69/CD1/1 (1998)

11. http://www-jt60.naka.jaea.go.jp/english/annual/04/html/contents.html

12. J. PAMELA, The physics of production, acceleration and neutralisation of large negative ion beams, Plasma Phys. and Contr. Fusion, 37, 325 (1995)

13. A.C.RIVIERE, Penetration of fast hydrogen atoms into a fusion reactor plasma, Nucl. Fus. 11, 363 (1971)

14. D.R. SWEETMAN Ignition condition in tokamak experiments and role of neutral injection heating, Nucl. Fus. 13, 157 (1973)

15. R.K. JANEV et al., Penetration of energetic neutral beamsinto fusion plasmas, Nucl. Fus. 29, 2125 (1989)

16. S.SUZUKI et al. Attenuation of high-energy neutral hydrogen beams in high-density plasmas, Plasma Phys. Contr. Fus., 40, 2097 (1998)

17. ITER team, et al., ITER Physics basis, Nucl. Fus. 39 (1999)

18. J.G. CORDEY, The neutral injection heating of toroidal plasmas to ignition, in Physics of Plasmas Close to Thermonuclear Conditions , EUR FU BRU/XII/476/80, Ed. CEC Brussels, I, 359 (1979)

19. D.V. SIVUKHIN, Coulomb collisions in a fully ionized plasma in Reviews of Plasma Physics, Ed. M.A. Leontovich, Consultants Bureau New York 4, 93 (1966)

20. C.F.F. KARNEY, Fokker-Planck and quasilinear codes, Computer Physics Reports 4, 183 (1986)

21. D. ANDERSON, Distortion of the distribution function of weakly RF heated minority ions in a tokamak plasma, J. Plasma Phys. 29, 317 (1983)

22. J.D.Jr. GAFFEY, Energetic ion distribution resulting from neutral beam injection in tokamaks, J. Plasma Phys. 16, 149 (1976)

23. D. VAN EESTER, Plasma heating and current drive: numerical methods, Second Carolus Magnus Summer School on Plasma Physics, Aachen 1995, Transactions of Fusion Technology, 29(1996) 258

24. R.J. GOLDSTON, Neutral beam injection experiments, Physics of Plasmas Close to Thermonuclear Conditions, EUR FU BRU/XII/476/80, Ed. CEC Brussels, II, 535 (1979)

25. W.W. HEIDBRINK et al., Comparison of experimental and theoretical fast ion slowing down times in DIII-D, Nucl. Fus. 28, 1897 (1988)

26. JET Team, Fusion energy production from a deuterium-tritium plasma in the JET tokamak, Nucl. Fus. 32, 187 (1992)

27. K. TOBITA, JT-60 Team, Latest plasma performance and experiments on JT-60U, Plasma Phys. and Contr. Fus., 41(1999) A333.

28. E. THOMPSON, et al., "The use of neutral beam heating to produce high performance fusion plasmas, including the injection of tritium beams into the Joint European torus (JET)", Phys. Fluids B, 5(1993) 2468

29. K. THOMSEN et al., ITER H mode confinement database update, Nucl. Fus. 34, 131, (1994)

30. J. JACQUINOT, JET Team, Deuterium-tritium operation in magnetic confinement experiments: results and underlying physics, Plasma Phys. and Contr. Fus., 41(1999)A13

31. K. IKEDA et al., Progress in the ITER physics basis, Nucl. Fus., 47, S1(2007)

32. S. GNTER, Overview of ASDEX Upgrade Results, et al., 20th Fusion Energy Conference, Vilamoura (2004) IAEA-CN-116 /OV/1-5

33. K. D. ZASTROW et al., Transfer rates of toroidal angular momentum during neutral beam injection, Nucl. Fus. 38, 257 (1998)

34. V.G. KIPTILY , et al., γ-ray diagnostics of energetic ions in JET, Nucl. Fus., 42, 999 (2002)

35. P.U. LAMALLE et al., Expanding the operating space of ICRF on JET with a view to ITER, Nucl. Fus., 46, 391, (2006) 391-400

36. Y.N. DNESTROWSKII & D.P. KOSTAMAROV, Numerical simulation of plasmas, Springer-Verlag (1986)

37. W.B. KUNKEL, Neutral beam injection, in Fusion Ed. E. Teller , Academic press 1B (1981)